Structures in the excitation function of $^{24}Mg(^{16}O,^{20}Ne)^{20}Ne$ and a nonresonant description of these structures

A. Lépine-Szily, R. Lichtenthäler Filho, M. M. Obuti, J. Martins de Oliveira, Jr., O. Portezan Filho, W. Sciani, and A. C. C. Villari*

Departamento de Física Nuclear, Instituto de Física da Universidade de São Paulo, 01498 São Paulo, São Paulo, Brazil

(Received 3 January 1989)

The excitation functions of the reactions $^{24}Mg(^{16}O,^{20}Ne)^{20}Ne$ and $^{24}Mg(^{16}O,^{12}C)^{28}Si$ were measured at $\theta_{c.m.}=90°$ and 70°, respectively, in the energy interval of 25 to 34 MeV in steps of 240 keV. They display strong structures with widths of 1 to 2 MeV and are compared to calculations including the coupling to higher orders between elastic and α-transfer channels, through the dynamic α-transfer polarization potential.

The anomalous back-angle behavior of the elastic scattering and α-transfer reactions between $n\alpha$-type nuclei have attracted considerable attention in the last decade.[1,2] The elastic scattering $^{24}Mg(^{16}O,^{16}O)^{24}Mg$ and the reaction $^{24}Mg(^{16}O,^{12}C)^{28}Si$ are good examples of this behavior, with a strongly oscillating backward increase in the angular distributions and highly structured excitation functions in forward and backward angles.[3–7]

We measured the excitation function of the reactions $^{24}Mg(^{16}O,^{20}Ne)^{20}Ne$ and $^{24}Mg(^{16}O,^{12}C)^{28}Si$, leading to ground states and first excited states in the final nuclei at $\theta_{c.m.}=90°\pm3°$ and $\theta_{c.m.}=70°\pm2.5°$, respectively, in the c.m. energy range from 25 to 34 MeV, with energy steps of 240 keV. Beams of ^{16}O were obtained from the São Paulo Pelletron Accelerator. We used isotopically enriched ^{24}Mg targets of 50 $\mu g/cm^2$, evaporated on carbon backing and containing a small amount of Bi. The outgoing particles were detected in kinematical coincidence by two surface-barrier Si detectors, placed at $\theta_{lab}=48.3°$ symmetrically with respect to the beam direction. The detection solid angle of 5 msr and the angular aperture of 3.5° ensured that in the coincidence spectra only the particles originating from the reactions $^{24}Mg(^{16}O,^{20}Ne)^{20}Ne$, $^{24}Mg(^{16}O,^{16}O)^{24}Mg$, and $^{24}Mg(^{16}O,^{12}C)^{28}Si$ were detected, avoiding all contaminant reactions; the energy resolution of the sum spectra E_1+E_2 was sufficient to allow the separation of peaks corresponding to ground and excited states in the reactions.

The efficiency of the kinematical coincidence method for each reaction was calculated by a Monte Carlo code,[8] which takes into account the size of the beam spot on the target and the detection solid angles. The elastic scattering $^{24}Mg(^{16}O,^{16}O)^{24}Mg$ had its efficiency measured by the simultaneous detection of the coincidence and free spectra, and the calculated efficiency agreed with the measured one within the statistical errors.

The excitation functions measured in this work for the reactions $^{24}Mg(^{16}O,^{20}Ne_{g.s.})^{20}Ne_{g.s.}$ at $\theta_{c.m.}=90°\pm3°$, $^{24}Mg[^{16}O,^{20}Ne(2^+)]^{20}Ne_{g.s.}$ at $\theta_{c.m.}=92°\pm3°$, $^{24}Mg(^{16}O,^{12}C)^{28}Si_{g.s.}$ at $\theta_{c.m.}=70°\pm2.5°$, and $^{24}Mg(^{16}O,^{12}C)^{28}Si(2^+)$ at $\theta_{c.m.}=71°\pm2.5°$ are shown in Fig. 1. They present oscillatory structures with widths of 1–2 MeV.

The excitation function of the reaction $^{24}Mg(^{16}O,^{20}Ne_{g.s.})^{20}Ne_{g.s.}$ at $\theta_{c.m.}=90°$ presents a strong minimum at $E_{c.m.}=27.8$ MeV. The angular distribution of this reaction at $E_{c.m.}=27.8$ MeV also presents a strong minimum[9] at $\theta_{c.m.}=90°$. The excitation functions of the reaction $^{24}Mg(^{16}O,^{12}C)^{28}Si_{g.s.}$ at $\theta_{c.m.}=0°$, 90°, and 180° present a prominent peak at the energy $E_{c.m.}=27.8$ MeV (see Fig. 2) which was interpreted[6] as an isolated resonance with $l=20$. The experimental minimum at 90° in the angular distribution[9] of the reaction $^{24}Mg(^{16}O,^{20}Ne)^{20}Ne$ seems in contradiction with the attribution of a single even l value, which should produce a maximum at 90° in the $^{20}Ne+^{20}Ne$ channel angular distribution.

The minimum at $\theta_{c.m.}=90°$ in the angular distribution of $^{24}Mg(^{16}O,^{20}Ne_{g.s.})^{20}Ne_{g.s.}$ can be fitted by the expression $|P_{18}(\cos\theta)+P_{20}(\cos\theta)|^2$, although the period of oscillations near 90° is not well reproduced.

Because of the presence of anomalies in both elastic and α-transfer reactions, an attractive explanation could be the coupling between elastic channel and the α-transfer channels.[9–12] The coupling to the α-transfer channel can be explicitly taken into account considering the dynamic α-transfer polarization potential[12] (DTPP), which describes the polarization of the two ions resulting from multiple α transfers. Details of the calculation can be found in Refs. 9 and 12. We have calculated[9] the effect of the DTPP on the elastic, inelastic, and α-transfer angular distributions of the following reaction channels at $E_{c.m.}=27.8$ MeV:

$^{24}Mg(^{16}O,^{16}O)^{24}Mg_{g.s.}$,

$^{24}Mg(^{16}O,^{16}O)^{24}Mg(2^+,1.37\ MeV)$,

$^{24}Mg(^{16}O,^{12}C)^{28}Si_{g.s.}$,

$^{24}Mg(^{16}O,^{12}C)^{28}Si(2^+,1.78\ MeV)$,

$^{24}Mg(^{16}O,^{20}Ne_{g.s.})^{20}Ne_{g.s.}$,

 ©1989 The American Physical Society

assuming the coupling between the elastic $^{24}Mg+^{16}O$ channel and the α-stripping channel $^{12}C+^{28}Si$. The effect of DTPP results in a back-angle increase in all angular distributions, with strong oscillations and reasonable agreement between experimental data and calculations.[9] However, the DTPP, which produces a sharply localized l window in the scattering matrix, also fails to explain the minimum at 90° in the $^{20}Ne+^{20}Ne$ channel angular distribution.

In the present work the DTPP was included in the calculation for the excitation functions of the reactions $^{24}Mg(^{16}O,^{12}C)^{28}Si$ and $^{24}Mg(^{16}O,^{20}Ne)^{20}Ne$, and some details of this calculation will be given below. The polarization potential V_{pol} can be written as[12]

$$V^l_{pol}(r)=C_l(E)F(r)\ , \tag{1}$$

where $F(r)$ is the form factor of the α-transfer reaction and $C_l(E)$ is given by

$$C_l(E)=A\left[-\frac{4i\mu_1}{\hbar^2 k_1}\frac{[I_l^{01}(k_0,k_1)]^2}{I_l^{00}(k_0)S^N_{l,1}(k_1)}\right]\ , \tag{2}$$

where I_l^{01} is the transfer radial integral, I_l^{00} is the elastic radial integral, and $S^N_{l,1}$ are the unperturbed nuclear elastic scattering matrix elements in the transfer channel.

We developed a distorted-wave Born approximation (DWBA) code, called DWPOL,[9] which calculates V_{pol} [Eq. (1)] and solves the Schrödinger equation with V_{pol} added to the optical potential, generating the exact elastic wave function. This exact wave function is used in DWPOL to calculate the elastic, inelastic, and α-transfer angular distributions. In order to estimate the effect of no-recoil (NR) and zero-range (ZR) approximations used in DWPOL, we compared the α-transfer differential cross sections calculated by DWPOL (without V_{pol}) and by the full finite range DWBA code PTOLEMY (Ref. 13) for the reactions $^{29}Mg(^{16}O,^{12}C)^{28}Si_{g.s.}$, $^{24}Mg(^{16}O,^{12}C)^{28}Si(2^+)$, $^{24}Mg(^{16}O,^{20}Ne_{g.s.})^{20}Ne_{g.s.}$, $^{24}Mg[^{16}O,^{20}Ne(2^+)]^{20}Ne_{g.s.}$ using the optical potentials *ANL*2 (Ref. 14) (Table I) and *PL*3*A* (Table I) in the incoming and outgoing channels. In the case of both potentials (*ANL*2 and *PL*3*A*), both calculations (ZR, NR, and full finite range) give very similar angular distributions for all of the above-mentioned reactions, resulting in the same constant normalization factor between DWPOL and PTOLEMY cross

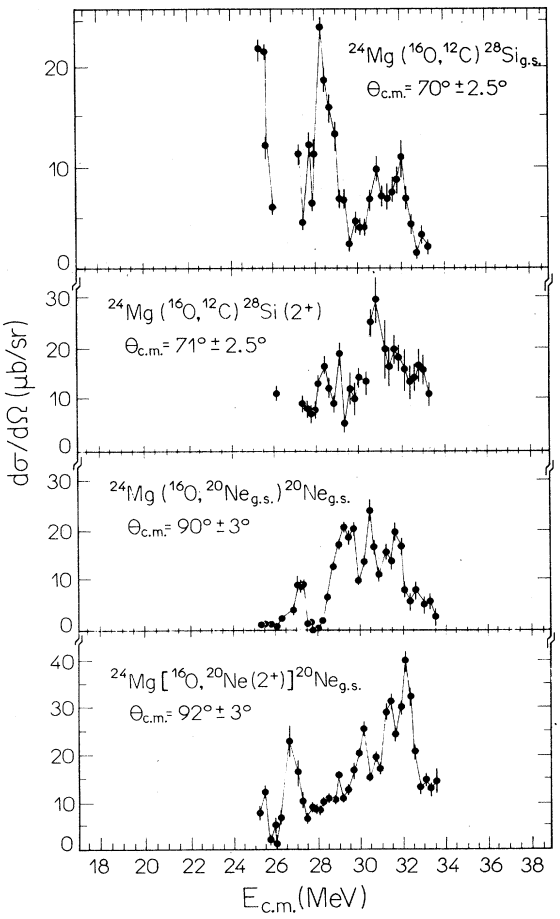

FIG. 1. Excitation functions for the indicated reactions. The solid lines connect the experimental points smoothly.

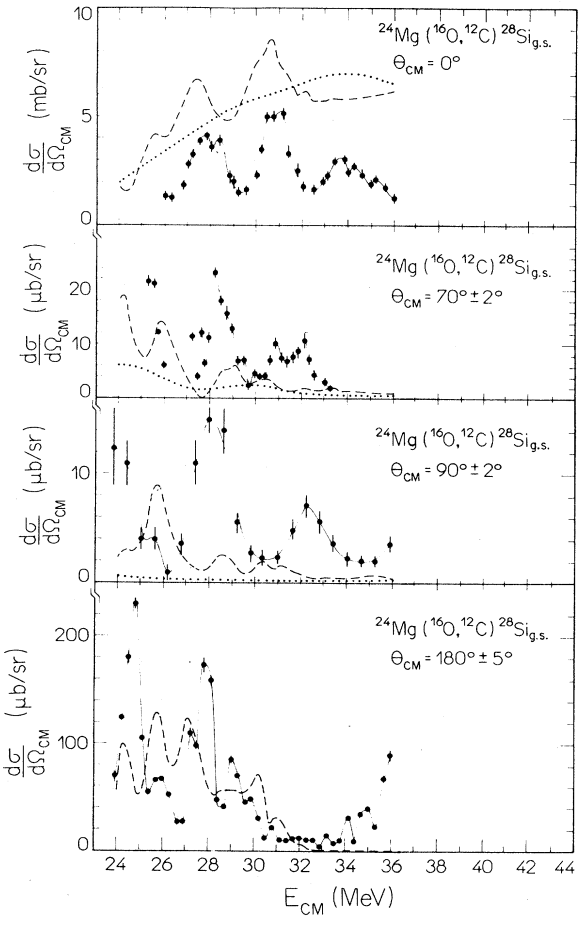

FIG. 2. Excitation functions for the indicated reactions. Our data were measured at 70°, the other data were obtained by the Argonne group (Ref. 6). Solid lines are to guide the eye. Dashed lines are the results of calculations including V_{pol}. Dotted line is the calculation without V_{pol}.

TABLE I. Optical potentials referred in the text.

Potential	V (MeV)	r_r (fm)	a_r (fm)	W (MeV)	r_I (fm)	a_I (fm)
ANL2	10.0	1.452	0.345	23.0	1.272	0.376
PL3A	10.0	1.452	0.345	30.0	1.252	0.376

sections. This normalization factor should multiply V_{pol} and the transfer cross sections to take into account the finite range and recoil effects. A slight modification of the imaginary part of potential *ANL2* resulted in the optical potential *PL3A*, which better reproduces the exit channel ($^{12}C+^{28}Si$) elastic angular distribution.

We performed calculations for the α-transfer excitation functions including V_{pol}, using the optical potential *ANL2* in the entrance channel and the potential *PL3A* in the exit channel. The excitation functions were obtained from angular distributions calculated at energies from 24 to 36 MeV in steps of 600 keV, averaging the cross sections in the angular range of detection. The optical-potential parameters were not varied in the whole energy range. The behavior of V_{pol} with energy is determined mainly by the radial integrals I_l^{01} and the S matrix $S_{l,1}^N$. It is important to note that V_{pol} varies smoothly with energy.

The wave function in the channel $^{20}Ne+^{20}Ne$ was symmetrized to take into account the identity of particles. The result of these calculations, compared with experimental excitation functions[6,9] of the reaction $^{24}Mg(^{16}O,^{12}C)^{28}Si_{g.s.}$ at $\theta_{c.m.}=0°$, 70°, 90°, and 180°, is shown in Fig. 2. The calculations compared with experimental excitation functions[9] of the reactions $^{24}Mg(^{16}O,^{20}Ne_{g.s.})^{20}Ne_{g.s.}$ at 90° and $^{24}Mg[^{16}O,^{20}Ne(2^+)]^{20}Ne_{g.s.}$ at 92° are shown in Fig. 3. The solid lines are to guide the eye through the experimental points, the dashed line is the result of calculations with V_{pol}, and the dotted line is the result without V_{pol}.

The effect of the inclusion of V_{pol} in the excitation functions has the following characteristics.

(a) The cross section of $^{24}Mg(^{16}O,^{12}C)^{28}Si_{g.s.}$ calculated without V_{pol} (dotted line in Fig. 2) at 0° is smoothly increasing with energy without any structure. The inclusion of V_{pol} produces structure in the excitation function with positions and widths comparable to the experimental structure.

(b) The cross section of the reaction $^{24}Mg(^{16}O,^{12}C)^{28}Si_{g.s.}$ calculated without V_{pol} at 180° is smoothly varying with energy and negligible when compared to experimental data. The inclusion of V_{pol} increases the cross section at 180° to the same order of magnitude as the experimental value, and produces structure whose widths are smaller than at 0° and comparable to the experimental widths. The general behavior at 180° with large peaks between 24 and 30 MeV and small cross section between 30 and 35 MeV is also reproduced by the calculation with V_{pol}.

(c) The experimental excitation functions of the reactions $^{24}Mg(^{16}O,^{20}Ne_{g.s.})^{20}Ne_{g.s.}$ and $^{24}Mg[^{16}O,^{20}Ne(2^+)]^{20}Ne_{g.s.}$ at 90° and 92°, respectively (Fig. 3) present structure with widths of 1 MeV, superimposed on a broad peak centered around 30 MeV. The calculations without V_{pol} yield again small, smoothly varying cross sections. The inclusion of V_{pol} produces the large peaks whose magnitudes, positions, and widths are comparable to the experimental ones. The strong minimum at 27.8 MeV is not obtained by the calculation with V_{pol}.

(d) The exact position of peaks is not reproduced by the calculation with V_{pol} and it depends on the optical potential used. Other calculations using different optical potentials, yield the same general behavior; the magnitude of the cross sections and the widths were maintained, with a variation in the position of the peaks.

Our calculations do not constitute a fit to the experimental excitation functions, but they show that the inclusion of the dynamic polarization of the interacting ions due to multiple α transfers producing prominent structure in the excitation functions of the α-transfer reactions at forward and backward angles, very similar in width and position to the experimental structure. We as-

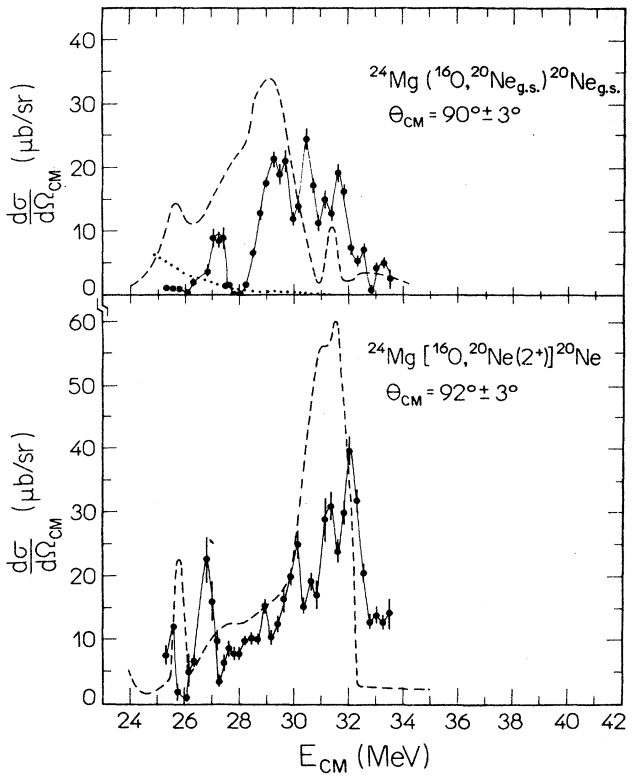

FIG. 3. Excitation functions for the indicated reactions. Solid lines are to guide the eye. Dashed line is the result of calculation with V_{pol} and dotted line without V_{pol}.

sumed a direct-reaction interpretation with multiple α transfers without any resonant process, and obtained strong peaks with general behavior comparable to the experimental data.

The large effect of V_{pol} is due to the inclusion of higher-order effects in the coupling, which produces a sharply localized deviation in l space and a large contribution at 180°. This was shown in a recent work,[15] where the effect on the elastic S matrix of the coupling to α-transfer channels was investigated for the system $^{16}O+^{28}Si$.

Our calculations have shown that the effect of V_{pol} decreases for increasing energy; at $E_{\text{c.m.}} > 35$ MeV the calculated cross sections for the reaction $^{24}Mg(^{16}O,^{12}C)^{28}Si_{\text{g.s.}}$ at 70°, 90°, and 180° become very low. The same result is obtained for $^{24}Mg(^{16}O,^{20}Ne)^{20}Ne$ at 90°. The multiple α transfers between channels $^{16}O+^{24}Mg$ and $^{12}C+^{28}Si$, described by V_{pol}, produce an enhancement in the backward angle transfer cross sections for a certain energy region, which can be understood even by semiclassical matching conditions. This "energy window" in the excitation function presents a broad peak around $E_{\text{c.m.}} = 28-30$ MeV with fine structures superimposed on it.

In conclusion, we have presented in this paper excitation function measurements for the channel $^{24}Mg(^{16}O,^{20}Ne)^{20}Ne$, and DTPP calculations for the excitation functions of the above reaction at 90°, and for the $^{24}Mg(^{16}O,^{12}C)^{28}Si_{\text{g.s.}}$ reaction at 0°, 70°, 90°, and 180°. The inclusion of the dynamic polarization of the interacting ions due to multiple α transfers produces prominent structures in the excitation functions of the α-transfer reactions at 0°, 90°, and 180°, very similar in width and position to the experimental structure. The excitation function in the $^{24}Mg(^{16}O,^{12}C)^{28}Si$ (2^+, 1.78 MeV) reaction at 180°, calculated with V_{pol}, also presents strong structures

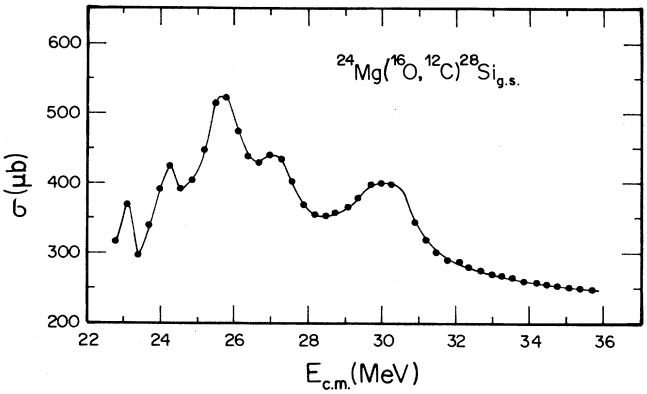

FIG. 4. Total angle-integrated transfer cross section of $^{24}Mg(^{16}O,^{12}C)^{28}Si_{\text{g.s.}}$, calculated with V_{pol}.

with widths similar to experimental ones. The structures also remain in the angle-integrated transfer cross sections of $^{24}Mg(^{16}O,^{12}C)^{28}Si_{\text{g.s.}}$, and $^{24}Mg(^{16}O,^{12}C)^{28}Si$ (2^+, 1.78 MeV) reactions, calculated with V_{pol} (see Fig. 4). This result agrees with experimental indications[6] about overall enhancement in the $^{24}Mg(^{16}O,^{12}C)^{28}Si_{\text{g.s.}}$ channel at $E_{\text{c.m.}} = 27.8$ MeV.

Our data and our DTPP calculations do not exclude the resonance interpretations, they offer an alternative nonresonant description, which also explains the anomalies observed in angular distributions,[9] excitations functions at several angles and even in the total angle-integrated excitation function.

This work was partially supported by the Conselho Nacional de Desenvolvimento Científico e Tecnologico (CNPq) and partially supported by Fundacão de Amparo a Pesquisa do Estado de São Paulo (FAPESP).

*Present address: Grand Accélérateur National d'Ions Lourds (GANIL), B.P. 5027, 14021 Caen, France.

[1]P. Braun-Munzinger and J. Barrette, Phys. Rep. **87**, 209 (1982), and references therein.

[2]J. Barrette and S. Kahana, Comment Nucl. Part. Phys. **9**, 67 (1980).

[3]M. Paul, S. J. Sanders, J. Cseh, D. F. Geeseman, W. Henning, D. G. Kovar, C. Olmer, and J. P. Schiffer, Phys. Rev. Lett. **40**, 1310 (1978).

[4]M. Paul, S. J. Sanders, D. F. Geeseman, W. Henning, D. G. Kovar, C. Olmer, J. P. Schiffer, J. Barrette, and M. J. Levine, Phys. Rev. C **21**, 1802 (1980).

[5]S. M. Lee, J. C. Adloff, P. Chevalier, D. Disdier, V. Rauch, and F. Scheibling, Phys. Rev. Lett. **42**, 429 (1979).

[6]S. J. Sanders, M. Paul, J. Cseh, D. F. Geeseman, W. Henning, D. G. Kovar, R. Kozub, C. Olmer, and J. P. Schiffer, Phys. Rev. C **21**, 1810 (1980).

[7]S. J. Sanders, H. Ernst, W. Henning, C. Jachcinski, D. G. Kovar, J. P. Schiffer, and J. Barrette, Phys. Rev. C **31**, 1775 (1985).

[8]V. H. Rotberg, Ph.D. thesis, University of São, Paulo, 1978.

[9]R. Lichtenthäler Filho, A. Lépine-Szily, A. C. C. Villari, and P. Portezan Filho, Phys. Rev. C **39**, 884 (1989).

[10]R. Lichtenthäler Filho, A. Lépine-Szily, A. C. C. Villari, W. Mitting, V. J. G. Porto, and C. V. Acquadro, Phys. Rev. C **26**, 2487 (1982).

[11]L. F. Canto, R. Donangelo, M. S. Hussein, and A. Lépine-Szily, Phys. Rev. Lett. **51**, 95 (1983).

[12]M. S. Hussein, A. N. Aleixo, L. F. Canto, P. Carrilho, R. Donangelo, and L. S. de Paula, J. Phys. G **13**, 967 (1987).

[13]M. H. Macfarlane and S. C. Pieper, Argonne National Laboratory Report ANL76-11 (unpublished).

[14]S. L. Tabor, D. F. Geeseman, W. Henning, D. G. Kovar, K. E. Rehm, and F. W. Prosser, Jr., Phys. Rev. C **17**, 2136 (1978).

[15]A. N. Aleixo, L. F. Canto, P. Carrilho, R. Donangelo, L. S. de Paula, and M. S. Hussein, Phys. Rev. C **37**, 1062 (1988).